Molecular packing and free volume in crosslinked epoxy networks

V. B. Gupta and C. Brahatheeswaran
Department of Textile Technology, Indian Institute of Technology, Delhi, New Delhi-110016, India
(Received 27 April 1990; revised 8 June 1990; accepted 19 June 1990)

A diglycidyl ether of bisphenol-A type difunctional epoxy resin was cured with different amounts of a tetrafunctional curing agent, namely metaphenylene diamine. The macrodensities of the cured samples were determined at room temperature and their volume expansion was measured from room temperature to 180°C using a dilatometer. By combining these data, specific volume–temperature plots were constructed. The occupied volume was determined either by extrapolating the specific volume to 0 K or by estimating the van der Waals volume for the network. The empty volume, packing coefficient and free volume fraction could then be calculated. It was observed that samples with a high degree of crosslinking showed good packing around 180°C but at the glass transition temperature (T_g) and in the glassy state, the packing was poor. It is postulated that after post-curing at 175°C, as the samples are allowed to cool, the constraints imposed by the crosslink affect the rate at which the samples contract; in samples with high crosslink density, the rate of contraction is subsequently low. Due to this, and also because of their high T_g, a larger free volume is trapped in these samples when the microbrownian motion freezes at T_g. With further cooling below T_g the intersegmental separation is relatively higher in the highly crosslinked samples because the crosslinks do not provide a suitable environment for close packing. The likely effects of molecular packing on physical properties are briefly considered.

(Keywords: epoxy network; crosslink density; packing coefficient; free volume; glass transition temperature)

INTRODUCTION

It is generally believed, on the basis of studies on vulcanized rubbers, that high crosslink density results in high macrodensity, high stiffness and low penetrant absorption. Various studies on crosslinked epoxy networks[1–10] suggest that high crosslink density can lead to low macrodensity, low stiffness and high penetrant absorption. It should be noted that these observations are related to the glassy state unlike vulcanized rubber, which is in the rubbery state. It is generally assumed[1–5] that these characteristics of epoxy networks are mainly due to the poorer packing of the molecules in the highly crosslinked samples, arising from constraints on the packing of molecules imposed by crosslinks. It has recently been suggested[11,12] that the decrease in macrodensity could arise from an increase of van der Waals volume resulting, for example, from the epoxide-amine addition reaction, and the packing coefficient would then increase with increase in crosslink density. Calculations based on more appropriate group contributions for oxygen[13,14], however, showed that the highly crosslinked samples have low packing coefficient. Since only very limited studies[15,16] have been made of the free volume in cured epoxy networks, it was considered worthwhile to undertake a more comprehensive characterization of the free volume with the aim of obtaining a clearer understanding of the structure–property correlations in these networks. The results of such a study are presented in this paper. The curing reactions[17], morphology[18], dynamic mechanical properties[4], tensile properties[19] and moisture absorption characteristics[20] of networks based on the same epoxy resin system have already been reported.

EXPERIMENTAL

Sample preparation

The epoxy resin used was Araldite GY 250 (Hindustan Ciba-Geigy Ltd), which is based on diglycidyl ether of bisphenol-A and has the chemical structure shown in *Formula A*.

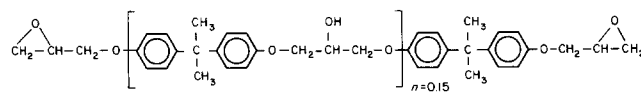

Formula A

The curing agent used was *meta*-phenylene diamine (mPDA) having the following chemical structure:

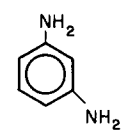

The curing agent concentration for the stoichiometric composition, i.e. one in which the ratio, P, of amine hydrogens [NH] to epoxy groups [E] is one to one, is calculated to be 14.5 parts by weight per hundred parts of the resin (phr) for this system. In the present investigations, samples were prepared containing 7.5, 10, 14.5, 20 and 25 phr of mPDA. The corresponding initial molar ratio of reactive groups, $P = [NH]/[E]$, for these five samples was 0.53, 0.71, 1.0, 1.42 and 1.77 respectively.

The following procedure was used for preparing the samples. The resin and the crosslinking agent were heated in separate containers in an oven set at 75°C until the mPDA melted. They were then mixed by stirring and the stirred mixture was vacuum-degassed for about 7 min

0032-3861/91/101875-10

before being poured into steel moulds to cast 2.5 mm thick sheets. Two curing cycles were used. 'Standard cure' (SC) samples were prepared by curing at 75°C for 2 h followed by 125°C for 2 h. 'Post-cure' (PC) samples were prepared by post-curing the SC samples at 175°C for 6 h in an inert gas environment.

Macrodensity

The densities of the cured samples were determined in a carbon tetrachloride–n-heptane density gradient column (Davenport). Four pieces of each sample were introduced into the column and allowed to settle. Readings were taken after 24 h. In each case, at least two readings were taken for two different sets of samples.

Crosslink density

The crosslink density was taken[21] to be equal to $(3M_c/2)^{-1}$, where M_c is the molecular weight between successive crosslinks and was determined from the rubbery torsional modulus (G') of these samples, using the following empirical expression[22]:

$$\log_{10} G' = 7 + \frac{293\rho}{M_c}$$

where ρ is the macrodensity. For the 7.5 phr sample, the torsional modulus values were taken from earlier work[4].

Specific volume

Standard Pyrex dilatometers with bulb and reservoir capacities of 2.5 and 10 cm^3 respectively and precision bore capillary tubing of 1 mm diameter were used to measure volume expansion of the cured resin sample. A small piece was cut from the sheet, dried, weighed and introduced into the dilatometer bulb which was then sealed. Double-distilled mercury was introduced into the reservoir which was then connected through a rubber tubing to a vacuum pump. On evacuating, the reservoir was slightly tilted so that the mercury could enter the bulb through the capillary. The bulb was then heated to 70°C to remove the last traces of trapped air. The volume expansion of mercury and of the glass dilatometer were measured separately using a silicone oil thermostat.

Volume expansions were measured from room temperature to 180°C at suitable intervals. At each temperature the sample was equilibrated for 20 min before taking the reading.

Since the weight of sample and its room temperature density were known, its volume at room temperature was known and this allowed specific volume of the sample to be determined at each temperature.

Glass transition temperature

The glass transition temperature was obtained from the specific volume–temperature data and also from the peak positions of the tan δ curves obtained during the dynamic torsional studies (not described here) using standard procedures.

Coefficient of volume thermal expansion

The volume thermal expansion coefficient, α, of an isotropic solid is given by:

$$\alpha = (1/V)\,(dV/dT)$$

where V is the specific volume and dV/dT is the slope of the specific volume–temperature curve. Since, for the present samples, the volume–temperature plots are composed of two linear regions below and above T_g, the thermal expansion coefficients in the glassy state (α_g) and in the rubbery state (α_r) could be determined at a particular temperature.

Compression factor

When epoxy resin reacts with mPDA, contraction takes place. The specific volume of the monomer mixture can be found from the rule of mixtures.

The compression factor, ΔV, may then be approximated[23] to the difference in volumes of the monomer mixture and the cured resin and is considered a sensitive characteristic of polymer packing. The calculations were made using the following values: molar volume of Araldite GY 250 = 327.36 cm^3; molar volume of mPDA = 94.93 cm^3; molar weight of Araldite GY 250 = 383.05 g; molar weight of mPDA = 108.14 g.

PARAMETERS CHARACTERIZING VOLUME AND MOLECULAR PACKING

The van der Waals volumes of the network

Standard cure (SC) samples. The van der Waals volume for the SC stoichiometric (14.5 phr) sample has been estimated[13], using the van der Waals volumes of the individual groups given by Bondi[24], to be 483.7 $cm^3\ mol^{-1}$. This value has been used in the present analysis.

The van der Waals volumes of the epoxy-rich SC samples (namely samples cured with 7.5 and 10.0 phr of curing agent) were estimated using the procedure described by Bellenger *et al.*[11]. For the amine-rich SC samples (namely samples cured with 20 and 25 phr of curing agent), the assumptions were made based on the observed reactions that take place[17]. For these samples it has been observed that all primary amines react relatively rapidly[17]. If the diamine is represented as $H_2N–A–NH_2$, where A is the phenylene group, then the van der Waals volume of the amine-rich sample (V_w) having y moles of excess amine over the stoichiometric amount will be given by:

$$V_w = V_w(S) + y[V_w(A) + 4V_w(NH) - 2V_w(N)]$$

where $V_w(S)$ and $V_w(A)$ are the van der Waals volumes of the stoichiometric sample and of the phenylene group respectively. For y moles of excess amine, there will be $2y$ moles of NH_2 group. Since all the epoxy groups are consumed, $4y$ moles of NH group will be left unreacted. Since the van der Waals volume of the two moles of nitrogen is already included in the $V_w(S)$ term, they have been subtracted and thus the above equation gives the van der Waals volumes of the amine-rich samples.

Post-cure (PC) samples. When the SC samples were post-cured, there were significant additional chemical reactions in the epoxy-rich samples[17]. In the stoichiometric and amine-rich samples, only minor changes took place. The van der Waals volumes for the PC stoichiometric and amine-rich samples were therefore taken to be the same as for the corresponding SC samples. For the epoxy-rich samples, if the sample is deficient by x moles of amine, then there will be $4x$ moles of unreacted epoxy groups. When these excess epoxy groups react with hydroxyl groups, a new hydroxyl group and an ether

link is formed. If a value of 3.7 $cm^3\ mol^{-1}$ is assigned for the newly formed ether oxygen[24], there will be a reduction of 0.75 $cm^3\ mol^{-1}$ for the reaction of every mole of epoxy group. The van der Waals volume of the epoxy-rich samples will thus be:

$$V_w = V_w(S) - x(4 \times 0.75)$$

Packing coefficient

The packing coefficient, ρ^*, is defined as the ratio of the van der Waals volume (V_w) of the structural unit to its molar volume (V_m), i.e.

$$\rho^* = V_w/V_m = V_w/(M/\rho)$$

where M is the molar weight of the structural unit and ρ is its macrodensity.

Empty volume

The thermal expansion or contraction of a solid in the glassy state is believed[25] to be related to the expansion or contraction of van der Waals volume, as a result of which the empty volume also changes as a function of temperature. The increase in van der Waals volume with temperature will be related to the volume fraction of the van der Waals volume and the rate at which specific volume changes in the glassy region. These considerations lead to the following relationship:

$$(V_w)_T = (V_w)_{T_r}[1 + (1/V_{T_r})(dV/dT)_g(T - T_r)]$$

where $(V_w)_T$ and $(V_w)_{T_r}$ are the specific van der Waals volumes at any temperature T and at room temperature, T_r, respectively, V_T is the specific volume at temperature T, and $(dV/dT)_g$ is the slope of the specific volume–temperature curve in the glassy state. The van der Waals volume was determined from room temperature to 180°C by the use of the above relationship.

The specific empty volume, V_E, was then taken as the difference between the measured specific volume, V, and the calculated specific van der Waals volume, V_w/M, i.e.

$$V_E = V - V_w/M$$

The empty volume fraction, $V_{f(E)}$, at any temperature was taken as the specific empty volume divided by the measured specific volume at that temperature, (V_E/V_T).

Doolittle free volume

The Doolittle free volume was taken as the excess of measured volume per mole at the temperature of interest over the molar volume at 0 K. The latter was estimated using the procedure suggested by Doolittle[26], namely by extrapolating the volume plot with temperature in the glassy state to 0 K. The free volume, $V_{(D)}$, is then defined as $V_{(D)} = V_T - V_0$, where V_0 is the volume occupied by the molecules per gram at 0 K under conditions of closest packing. The fractional free volume, $V_{f(D)}$, is then given by $(V_T - V_0)/V_T$.

Simha–Boyer free volume fraction at T_g

If the expansion coefficients above and below T_g are α_r and α_g respectively, then according to Simha and Boyer[27], the factor $(\alpha_r - \alpha_g)T_g$, where T_g is in K, is a constant for amorphous polymers (around 0.113) and provides a measure of the free volume fraction, $V_{f(S-B)}$, at T_g.

Williams–Landel–Ferry (WLF) free volume fraction at T_g

According to the WLF treatment[28,29], the free volume fraction at T_g is related to the shift factor, log a_T, which was found from the dynamic torsional modulus data over a range of frequency and temperature on a similar system[4]. Taking the T_g of the sample as the reference temperature for constructing the master curve, plots of $(T - T_g)/\log a_T$ *versus* $(T - T_g)$ give the slope which is a constant (C_1) of the WLF equation. The free volume fraction, $V_{f(WLF)}$, is then given by $1/(2.303C_1)$.

The frozen fraction

Simha and Wilson[30] have defined a frozen fraction (FF) in amorphous polymers which has an inverse relationship with the hole fraction. Since low T_g systems are expected to require relatively few holes to pass into the liquid state, the hole fraction at T_g cannot be constant. The correlation of frozen fraction with T_g for a number of amorphous polymers led to the following empirical relationship, which can be used for determining the frozen fraction:

$$FF = 1.107 - (1.346 \times 10^{-3} \times T_g)$$

where T_g is in K.

RESULTS AND DISCUSSION

Sample characteristics

Molecular weight between crosslinks and crosslink density. The values of M_c, the molecular weight between successive crosslinks, determined from the values of rubbery torsional modulus (not reported here) for the samples of different stoichiometry are shown in *Figure 1a* while the crosslink density data for the same samples is presented in *Figure 1b*. As expected, the stoichiometric sample has the lowest M_c and the highest crosslink density amongst the standard cure samples and on either side of stoichiometry, crosslink density decreases. Post-curing results in considerable increase in the crosslink density of the epoxy-rich samples, but the effect on the other samples is very slight. Since the post-cure samples are more fully cured, their chemistry would be expected to remain essentially unchanged during thermal exposure and therefore the bulk of the discussion concerns these samples. However, as shown earlier[20], the 7.5 phr post-cure sample showed some signs of damage when exposed to 100% relative humidity at 125°C, which appeared mainly as elliptical voids with major axes in the range 10–15 μm. Data on this sample has therefore not been included in all cases.

Room temperature macrodensity and compression factor. The room temperature macrodensity data, as obtained from measurements on a density gradient column, is presented in *Figure 2*. Samples with the highest crosslink density have the lowest macrodensity at room temperature. On post-curing, the macrodensities of all the standard cure samples decrease, the largest decrease being for the 10 phr sample.

The compression factor data, presented in *Table 1*, shows that on curing, the monomer mixture undergoes the least contraction in the case of the samples with the highest crosslink density. This is apparently due to the constraints imposed on molecular packing by the crosslinks.

The van der Waals volume. The van der Waals volumes, V_w, for the networks were calculated by using the procedure described earlier. For oxygen, the following V_w values were used[13]: 5.5 $cm^3\ mol^{-1}$ for epoxide oxygen; 3.2 $cm^3\ mol^{-1}$ for phenylene oxygen; and 3.7 $cm^3\ mol^{-1}$ for ether linkage which is formed by the reaction between the epoxy and –OH groups[17]. The justification for using these values has been discussed in an earlier publication[13]. The data for the post-cure samples are shown in *Table 2*. Also included in the table, for reference, are the room temperature specific volume values obtained from the macrodensity data. It is noteworthy that the van der Waals volume increases with increase in mPDA content, since V_w per gram of mPDA is higher than the corresponding V_w per gram of epoxy prepolymer. The specific volume, on the other hand, shows a maximum for the sample with the highest crosslink density.

Specific volume. The specific volume data for the post-cure samples from room temperature to 180°C is presented in *Figure 3*. It is observed that the volume–temperature relationship is linear with the slope below T_g being much lower than the slope above T_g. Also, the most highly crosslinked samples with the highest T_g have the highest specific volume at and below T_g and the lowest at around 180°C.

Glass transition temperature. The glass transition temperature of the post-cure samples, as obtained from the peak positions of tan δ on the torsion pendulum at a frequency of about 1 Hz and from the dilatometer data, are shown in *Figure 4*. As expected, the T_g values of the highly crosslinked samples are the highest; on either side of stoichiometry T_g decreases. The difference in the T_g values obtained by the two methods is also as expected.

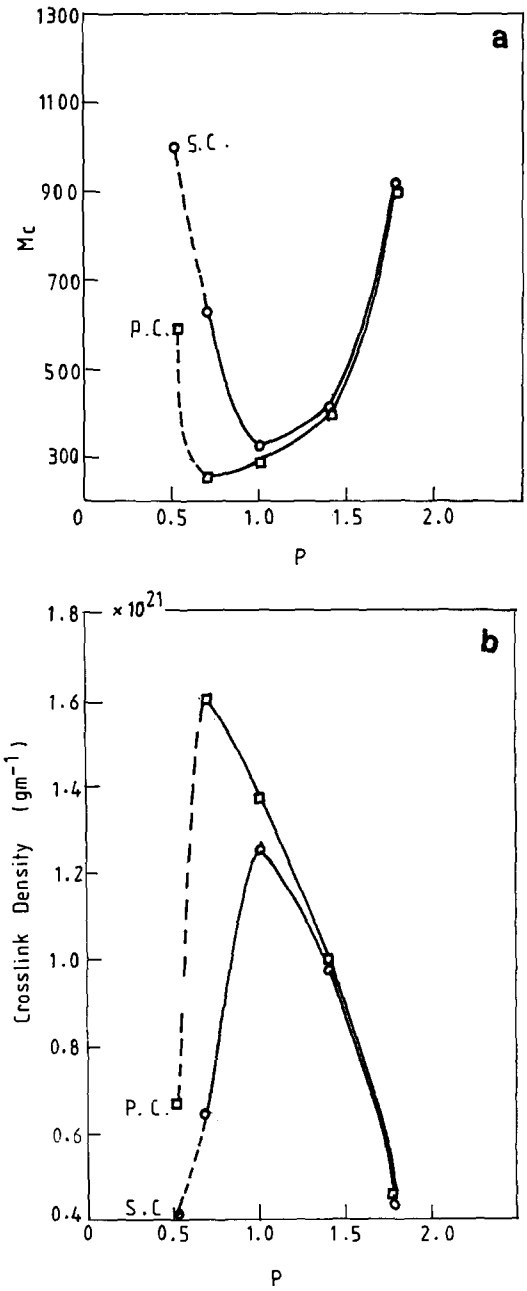

Figure 1 (a) Molecular weight between crosslinks (M_c) and (b) crosslink density data for standard cure (SC) and post-cure (PC) samples prepared using different initial molar ratio of reactive groups, $P = [NH]/[E]$

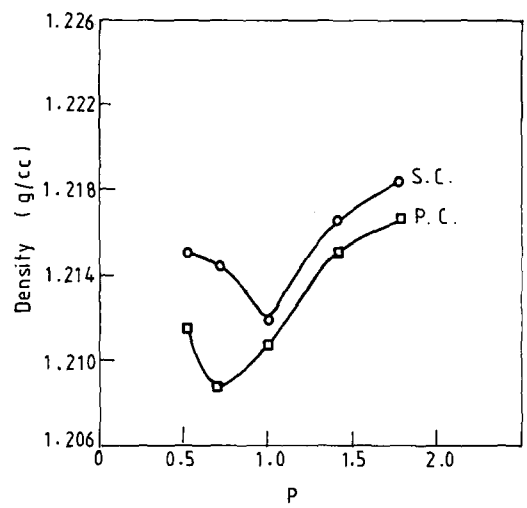

Figure 2 Room temperature density values for standard cure (SC) and post-cure (PC) samples prepared using different initial molar ratio of reactive groups, $P = [NH]/[E]$

Table 1 Room temperature compression factor data

mPDA (phr)	Specific volume of monomer mixture ($cm^3\ g^{-1}$)	Standard cure samples		Post-cure samples	
		Specific volume ($cm^3\ g^{-1}$)	Compression factor ($cm^3\ g^{-1}$)	Specific volume ($cm^3\ g^{-1}$)	Compression factor ($cm^3\ g^{-1}$)
7.5	0.8562	0.8230	0.0332	0.8255	0.0307
10.0	0.8567	0.8235	0.0332	0.8275	0.0292
14.5	0.8575	0.8252	0.0323	0.8260	0.0315
20.0	0.8585	0.8220	0.0365	0.8230	0.0355
25.0	0.8593	0.8207	0.0386	0.8220	0.0373

Table 2 The van der Waals volumes of post-cure samples

mPDA (phr)	V_w ($cm^3\ mol^{-1}$)	M ($g\ mol^{-1}$)	V_w/M ($cm^3\ g^{-1}$)	Specific volume at room temperature ($cm^3\ g^{-1}$)
7.5	453.9	823.4	0.5513	0.8255
10.0	465.2	842.5	0.5522	0.8275
14.5	483.7	874.2	0.5533	0.8260
20.0	511.6	919.3	0.5565	0.8230
25.0	535.6	957.6	0.5590	0.8220

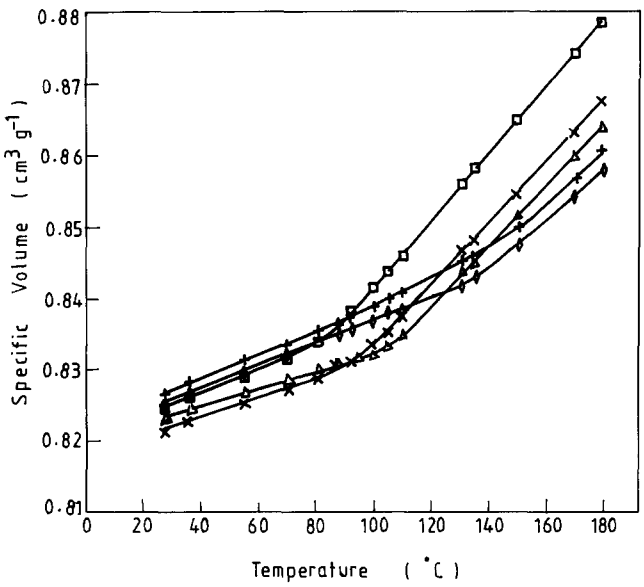

Figure 3 Specific volume as a function of temperature for post-cured epoxy resin samples prepared using different initial molar ratio of reactive groups. Concentration of mPDA (phr): □, 7.5; +, 10.0; ◇, 14.5; △, 20.0; ×, 25.0

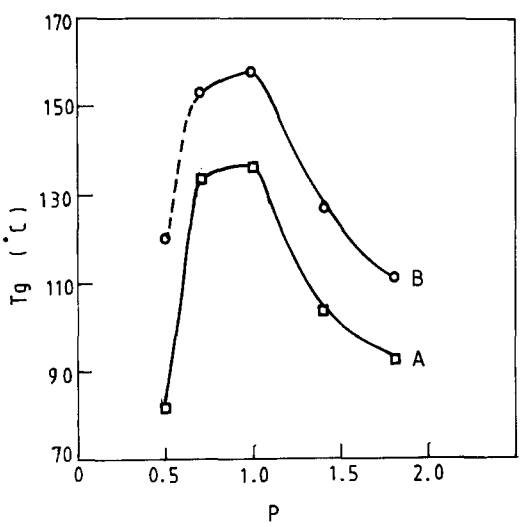

Figure 4 Glass transition temperatures of the post-cure samples prepared using different initial molar ratio of reactive groups, $P = [NH]/[E]$. Curve A, from dilatometer studies, curve B, from tan δ peak in torsion

Thermal expansion characteristics. The slopes of the specific volume–temperature plots in the glassy and rubbery states were estimated and are shown in *Table 3*. It is noteworthy that while above T_g the highly crosslinked samples show the smallest thermal expansion,

Table 3 The slopes of the specific volume–temperature plots in the glassy, $(dV/dT)_g$, and rubbery, $(dV/dT)_r$, states

mPDA (phr)	$(dV/dT)_g$ ($10^{-4}\ cm^3\ °C^{-1}$)	$(dV/dT)_r$ ($10^{-4}\ cm^3\ °C^{-1}$)
7.5	1.48	4.60
10.0	1.61	3.55
14.5	1.56	3.50
20.0	1.49	4.15
25.0	1.38	4.35

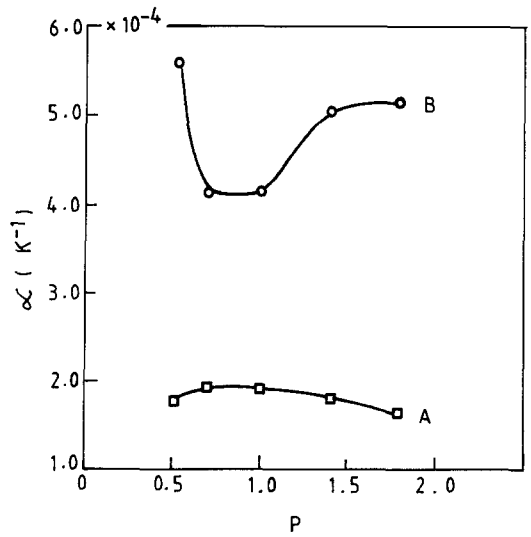

Figure 5 Volumetric expansion coefficient (α) for post-cure samples prepared using different initial molar ratio of reactive group, $P = [NH]/[E]$. Curve A, in the glassy state (α_g) and Curve B, in the rubbery state (α_r)

below T_g they show the highest. It may be seen from *Figure 5* that $(\alpha_r - \alpha_g)$ has the smallest value for the most highly crosslinked samples.

It is known that below T_g the glass expands with increasing temperature due to the normal expansion processes of all molecules which result from the changing vibrational amplitude of their constituents. Above T_g, in addition to the normal process, there will be an expansion of the free volume itself which will result in a larger expansion of the rubber than of the glass, the rubbery thermal expansion being around two to three times the glassy expansion.

Packing coefficient and empty volume. The data on packing coefficient, ρ^*, and empty volume, V_E, are presented in *Figures 6* and *7* respectively. In the glassy state the most highly crosslinked samples have higher empty volume and lower packing coefficient while at the highest temperatures studied, the situation reverses.

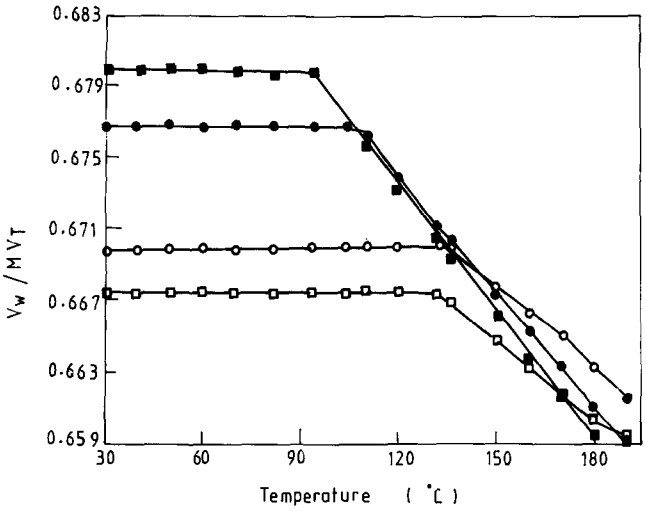

Figure 6 Packing coefficient as a function of temperature for post-cured epoxy resin samples prepared using different initial molar ratio of reactive groups. Concentration of mPDA (phr): □, 10.0; ○, 14.5; ●, 20.0; ■, 25.0

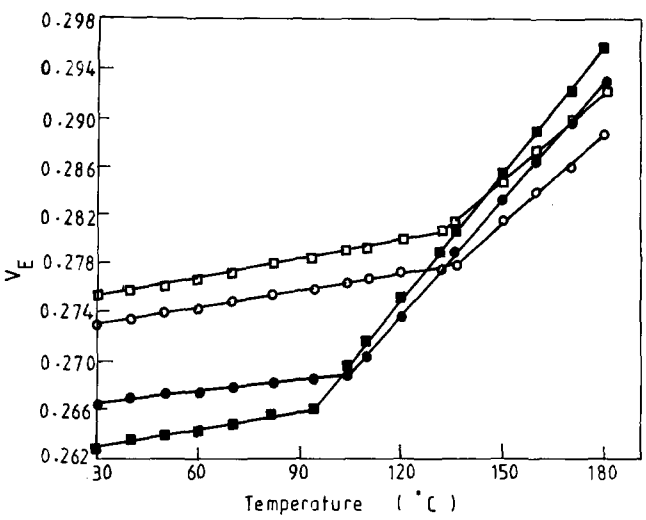

Figure 7 Empty volume as a function of temperature for post-cured epoxy resin samples prepared using different initial molar ratio of reactive groups. Symbols as in *Figure 6*

Doolittle free volume. The temperature dependence of Doolittle free volume fraction is shown in *Figure 8*. At high temperatures the free volume is lowest in the highly crosslinked samples while it is highest in the glassy state. This reversal in free volume in going from 180°C to room temperature is similar to the reversal in specific volume (*Figure 3*) and in packing coefficient (*Figure 6*).

The WLF and Simha–Boyer free volume at T_g. The free volume fractions at T_g, obtained using the WLF and Simha–Boyer approaches, are shown in *Table 4*. On both these schemes, the most highly crosslinked samples have the lowest free volume at T_g. It may be noted that this result does not appear to be in line with the other schemes.

The frozen fraction. The values of frozen fraction (FF) and the mobile fraction (1 − FF) are given in *Table 5*. It is interesting to note that the most highly crosslinked samples have a relatively higher mobile fraction, suggesting that they have more free volume.

Analysis of the data

An overview. The parameters characterizing molecular packing and free volume have been tabulated in *Table 6* for the various samples studied at three temperatures, i.e. at 180°C, at T_g and at 30°C. The Simha–Boyer and WLF free volume fractions were determined at T_g as described earlier and were assumed to remain constant below T_g. Above T_g, the following linear equation was used for the Simha–Boyer case:

$$(V_{S-B})_T = (V_{S-B})_{T_g} + [(dV/dT)_r - (dV/dT)_g](T - T_g)$$

Similarly the WLF free volume could be determined at higher temperatures.

At and around 180°C, the total specific volume (V_T), the empty volume fraction, ($V_{f(E)}$), the Doolittle free volume fraction ($V_{f(D)}$), the Simha–Boyer free volume fraction ($V_{f(S-B)}$), and the WLF free volume fraction ($V_{f(WLF)}$) all have the smallest value for the most highly crosslinked samples while the packing coefficient (ρ^*) has

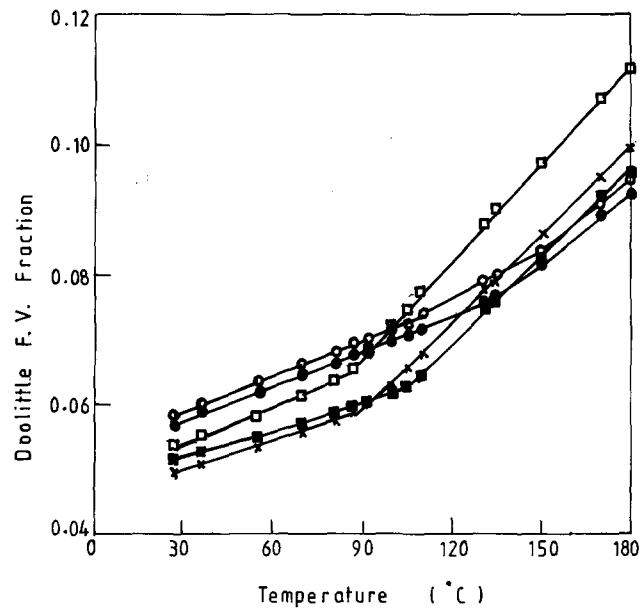

Figure 8 Doolittle free volume fraction as a function of temperature for post-cured epoxy resin samples prepared using different initial molar ratio of reactive groups. Concentration of mPDA (phr): □, 7.5; ○, 10.0; ●, 14.5; ■, 20.0; ×, 25.0

Table 4 The WLF and Simha–Boyer free volume fractions at T_g in the post-cure samples

mPDA (phr)	$V_{f(WLF)}$	$V_{f(S-B)}$
7.5	0.02	0.137
10.0	0.017	0.091
14.5	0.017	0.093
20.0	0.034	0.127
25.0	0.028	0.129

Table 5 The frozen and mobile fractions in the post-cure samples at T_g

mPDA (phr)	Frozen fraction	Mobile fraction
7.5	0.631	0.369
10.0	0.563	0.437
14.5	0.558	0.442
20.0	0.598	0.402
25.0	0.616	0.384

Table 6 Parameters characterizing molecular packing and free volume in cured epoxy networks (see text for symbols)

	Curing agent concentration (phr)				
	7.5	10.0	14.5	20.0	25.0
Dilatometric					
T_g (°C)	82	132.5	136	105	93
At 180°C					
V_T (cm^3 g^{-1})	0.8793	0.8605	0.8580	0.8643	0.8685
$V_{f(E)}$	0.3564	0.3396	0.3367	0.3389	0.3405
ρ^*	0.6436	0.6604	0.6633	0.6611	0.6595
$V_{f(D)}$	0.1119	0.0949	0.0920	0.0983	0.1014
$V_{f(S-B)}$	0.1653	0.0994	0.1018	0.1421	0.1522
$V_{f(WLF)}$	0.0547	0.0271	0.0268	0.0562	0.0557
At T_g					
V_T (cm^3 g^{-1})	0.8330	0.8435	0.8425	0.8330	0.8310
$V_{f(E)}$	0.3321	0.3326	0.3300	0.3230	0.3203
ρ^*	0.6679	0.6674	0.6700	0.6770	0.6797
$V_{f(D)}$	0.0625	0.0767	0.6567	0.6681	0.6727
$V_{f(S-B)}$	0.1368	0.0907	0.0934	0.1231	0.1288
$V_{f(WLF)}$	0.02	0.017	0.017	0.034	0.0280
At 30°C					
V_T (cm^3 g^{-1})	0.8255	0.8275	0.8260	0.8230	0.8220
$V_{f(E)}$	0.3323	0.3327	0.3301	0.3238	0.3200
ρ^*	0.6678	0.6673	0.6699	0.6762	0.6800
$V_{f(D)}$	0.0540	0.0589	0.0568	0.0531	0.0506
$V_{f(S-B)}$	0.1380	0.0925	0.0953	0.1246	0.1302
$V_{f(WLF)}$	0.0202	0.0173	0.0173	0.0344	0.0283

its highest value. Thus in the high temperature region, the most highly crosslinked samples are the most tightly packed. This is apparently because at these temperatures, when the microbrownian motion is intense, the crosslinks impose a constraint on intermolecular separation and so restrict motion.

The situation at T_g and at 30°C is the reverse of that at 180°C as far as the total specific volume, the empty volume fraction, the Doolittle free volume fraction and the packing coefficient are concerned, as they all suggest that the most highly crosslinked network is the most loosely packed. In addition to these parameters, the frozen fraction at T_g (*Table 5*) and the compression factor at room temperature (*Table 1*) also support the same conclusion. However, the values of Simha–Boyer and WLF free volume fractions (*Table 4*) tend to suggest that at and below T_g, the most highly crosslinked network is the most tightly packed as at 180°C. To resolve the conflict between these results and the earlier data, the concept of free volume needs to be examined.

The concept of free volume. The spatial distribution of free volume of a polymer in the rubbery or liquid state has been visualized[31,32] as being partly discontinuous (holes) and partly accommodated by an increase in the minimum interatomic spacing. In the original hole theory of liquids developed by Eyring and his associates[33,34], the latter is neglected and the discontinuous free volume is attributed entirely to the formation of holes which have to be treated simply as abnormal gaps in the structure which arise and collapse spontaneously. In general, when an amorphous polymer is allowed to cool from above T_g into the glassy state, the free energy would be expected to be dependent on sample volume through two variables, namely the average intersegmental distance between neighbouring chains in the close-packed regions of the sample and the number and size of holes present. The former factor is concerned mainly with internal energy and the latter with entropy. Above T_g the actual volume of the sample adjusts itself and acquires a particular intersegmental separation and a specific number and size distribution of holes to minimize the free energy level. Below T_g the segmental rotation becomes frozen and the holes which are present at T_g become immobilized. Thus the distribution of chain segments and free volume at T_g, which represents the equilibrium distribution at that temperature, must be retained at all temperatures below T_g. On cooling the sample below T_g the most frequently stated view is that the free volume of the sample cannot decrease rapidly as the holes are no longer able to diffuse out of the structure. However, the intersegmental separation in the close-packed regions can adjust itself below T_g as the thermal vibrations of the atoms become reduced.

The thermal expansion characteristics. Based on the above discussion, it would be expected that above T_g the holes will dominate the free volume while below T_g the intersegmental separation will be important. The thermal expansion coefficients in the two regions clearly indicate that in the rubbery state, when the kinetic elements of neighbouring chains have considerable mobility, the crosslinks prevent adjacent chains from moving too far away from one another[35]. The rate of expansion during heating or of contraction during cooling, is therefore the

smallest in the most highly crosslinked samples. Since the α-transition in epoxy networks is believed[36] to involve the rotation of the segments between crosslinks, the moving segment will be relatively smaller in the most highly crosslinked samples than in samples with lower crosslink density. However, since the constraints to movement imposed by crosslinks are large in the highly crosslinked samples, the activation energy for α-relaxation is higher by a factor of two for the highly crosslinked samples[4]. Also, the number of segments between crosslinks will be the largest in highly crosslinked samples. Thus it would be expected that in the highly crosslinked samples there would be a large number of small holes while in the samples with low crosslink density, there would be a smaller number of larger holes.

In the light of the above discussion, the observation that the most highly crosslinked samples with a tighter network at 180°C have the highest free volume at T_g can be traced to the following two considerations. First, as these samples move to lower temperatures, the closing of the holes due to reduced microbrownian motion is at a slower rate compared to that for a less crosslinked sample. Second, in these highly crosslinked samples with high T_g, the microbrownian motion is quenched at a relatively higher temperature. Consequently more free volume is 'trapped' in these samples at T_g.

With further reduction in temperature, in the absence of large scale segmental motion, the contraction characteristics are reversed, the most highly crosslinked samples now showing the highest rate of contraction. In the glassy state the thermal motion is restricted to the relaxation mechanisms available at β relaxation, namely the motion of the smaller hydroxy ether groups[4] or to the crosslinks themselves[4,37] which can move because of the relatively higher free volume. Thus the highly crosslinked samples with greater number of crosslinks contract at a slightly higher rate compared to samples of low crosslink density. The intersegmental separation, however, is still the largest in these samples, as has been demonstrated by wide-angle X-ray diffraction studies on similar samples[38].

Free volume distribution. The lack of consistency amongst the approaches used to characterize free volume can now be attributed, following Struik[39], to the problem of quantifying the free volume and defining it in terms of measurable quantities. Cohen and Turnbull[40] emphasized that out of the total free volume formed from a number of holes of varying sizes, only a few large holes contribute to mobility. Thus the average free volume may not be a good measure of mobility. As shown in *Table 6*, the free and empty volume fractions at T_g obtained for the five samples using different approaches, are quite different. The WLF approach gives free volume fraction in the range 0.02–0.04 while Doolittle's method gives values in the range 0.05–0.11. The van der Waals volume calculations lead to an empty volume fraction of around 0.34 while the frozen fraction approach gives mobile fractions in the range 0.37–0.44. Other approaches have been suggested[41–43] for determining the free volume fraction at T_g; one of these[41], based on cooperative movements between a number of segments, leads to a universal value of 0.20. Thus there is a need to understand the basis for the wide variation in these values.

It has been suggested by Litt[42] that the WLF free volume fraction (0.02–0.04) is a measure of the effective free volume representing the larger holes which make segmental relaxation possible. The larger values (0.30–0.40) obtained in the present analysis are obviously measures of the total free space available while the intermediate values (0.10–0.20) are apparently measures of varying hole sizes. In this sense, the WLF free volume is consistent with the other free volume data in that though it leads to the smallest free volume fraction at and below T_g for the most highly crosslinked samples, this free volume is made up of only large holes. The Simha–Boyer free volume fraction would also perhaps be more representative of the larger holes in view of the fact that it is based on extrapolation of the rubbery part of the specific volume–temperature curve to 0 K. As shown in *Table 7*, the occupied volumes obtained by this method for the highly crosslinked samples are high; the high values apparently arise from the lower slope of the rubbery part of the curve. Moreover these values are not consistent with the trend shown by the values calculated by the other two methods and they are much higher than the WLF values, therefore they merit further examination.

The Simha–Boyer free volume. The Simha–Boyer free volume expression can be written as:

$$(\alpha_r - \alpha_g) = (V_{(S-B)}/V_{T_g})(1/T_g)$$

where $V_{(S-B)}$ is the Simha–Boyer free volume and V_{T_g} the specific volume at T_g. Based on the data for a large number of amorphous polymers, it has been shown[43–45] that when $(\alpha_r - \alpha_g)$ is plotted as a function of $1/T_g$, a straight line with a slope of 0.113 is obtained, which is therefore considered to be the universal free volume fraction at T_g. However, there are small deviations from the universal line; for a number of polymers the values range from 0.08 to 0.13 and have been attributed to additional molecular processes such as side chain motion. When the data are plotted for the present samples and for five other samples of crosslinked epoxy networks, for which data are available in the literature[36], they do not fall on the universal line (*Figure 9*) and the values also show a large scatter, being in the range 0.09–0.14 for the five samples studied and 0.07–0.13 for the five samples from the literature. For these samples the slope is high, i.e. for the present five samples it is around 0.37. This clearly suggests that the Simha–Boyer approach in its present form would not be expected to be a representative of the free volume in epoxy networks. It has also been pointed out[45,46] that the predictions based on this rule must be treated with reserve. Thus it may be concluded that the various measures of free volume and empty volume used in the present analysis provide a reasonably consistent framework in support of the free volume approach.

Supporting evidence for the free volume approach. There is considerable further evidence in the literature to

Table 7 The occupied volumes (V_0) obtained by the three methods described in the text

mPDA (phr)	V_w ($cm^3\ g^{-1}$)	$V_{0(S-B)}$ ($cm^3\ g^{-1}$)	$V_{0(D)}$ ($cm^3\ g^{-1}$)
7.5	0.5513	0.6669	0.7809
10.0	0.5522	0.7018	0.7788
14.5	0.5533	0.6985	0.7791
20.0	0.5565	0.6754	0.7793
25.0	0.5590	0.6743	0.7804

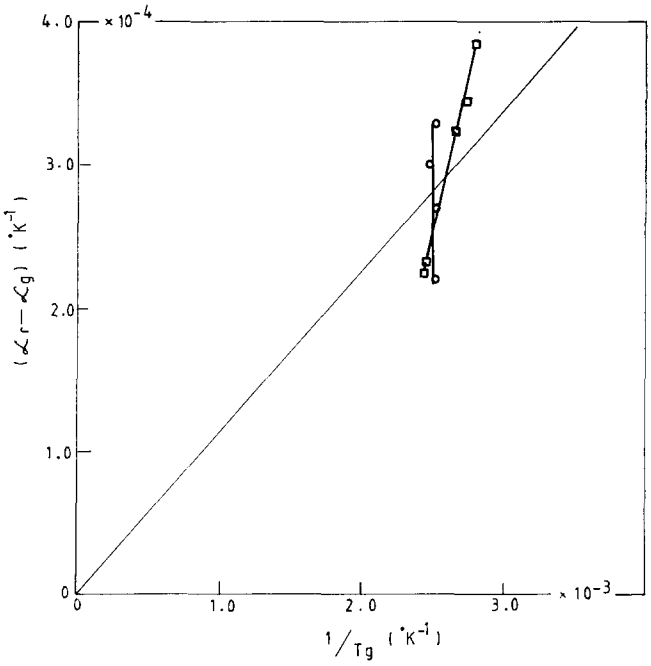

Figure 9 The Simha–Boyer universal plot for polymers (diagonal line through origin). The points for the present post-cured samples prepared using different initial molar ratio of reactive groups (□) and for samples reported in ref. 36 (○) are also shown

support the basic approach that in highly crosslinked epoxy networks based on rigid prepolymers, there is relatively more free volume. This evidence derives from elastic modulus data at room temperature[7,8,19], moisture absorption studies[16,20,47,48] over a range of temperature and ageing studies on epoxy networks[16].

It has been stated[21] that in samples in which differences in crosslink density arise from changes in stoichiometry, the role of chemical structure could also play an important role. There are a number of examples in the literature[1,2,16,49–51] of stoichiometric samples with different degrees of crosslink density which show characteristics similar to the post-cure samples of the present study in that the most highly crosslinked samples have the lowest density or the highest free volume content at T_g and at room temperature. It has been shown[15] that the role of chemical structure is only subsidiary in these cases.

CONCLUSIONS

From a detailed characterization of the free volume in crosslinked epoxy networks based on a rigid prepolymer and curing agent presented in this paper, it can be concluded that the samples with high crosslink density have relatively higher free volume at and below T_g because the crosslink site does not provide a suitable environment for close packing of the rigid molecules. It has also been postulated that in the highly crosslinked samples, the free volume distribution is made up of a large number of relatively smaller holes. Each crosslink site has more free volume, with the result that in the glassy state there is more likelihood of motion of crosslinks which results in high glassy thermal expansion of the highly crosslinked samples. Finally, the Simha–Boyer free volume is shown to be inadequate for characterizing the free volume in these networks.

ACKNOWLEDGEMENTS

The assistance of Dr Satish Kumar of Georgia Institute of Technology, USA in calculating the WLF free volume fractions and useful discussions with Dr E. F. T. White of UMIST, Manchester, UK are gratefully acknowledged.

REFERENCES

1 Kinjo, N., Ogata, M., Nishi, K. and Kaneda, A. *Adv. Polym. Sci.* 1988, **88**, 1
2 Pang, K. P. and Gillham, J. K. *J. Appl. Polym. Sci.* 1989, **37**, 1969
3 Morgan, R. J., Kong, F.-M. and Walkup, C. M. *Polymer* 1984, **25**, 375
4 Gupta, V. B., Drzal, L. T., Lee, C. Y.-C. and Rich, M. J. *J. Macromol. Sci.-Phys.* 1984–85, **B23**, 435
5 Enns, J. B. and Gillham, J. K. *J. Appl. Polym. Sci.* 1983, **28**, 2831
6 Findley, W. N. and Reed, R. M. *Polym. Eng. Sci.* 1977, **17**, 837
7 Selby, K. and Miller, L. E. *J. Mat. Sci.* 1975, **10**, 12
8 Kim, S. L., Skibo, M. D., Manson, J. A., Hertzberg, B. W. and Janiszewski, J. *Polym. Eng. Sci.* 1978, **18**, 1093
9 Barton, J. M. *Polymer* 1979, **20**, 1019
10 Gordon, G. A. and Ravve, A. *Polym. Eng. Sci.* 1980, **20**, 70
11 Bellenger, V., Dhaoui, W. and Verdu, J. *J. Appl. Polym. Sci.* 1987, **33**, 2647
12 Bellenger, V., Dhaoui, W., Morel, E. and Verdu, J. *J. Appl. Polym. Sci.* 1988, **35**, 563
13 Gupta, V. B. and Brahatheeswaran, C. *J. Appl. Polym. Sci.* 1989, **38**, 1957
14 Gupta, V. B. and Brahatheeswaran, C. *J. Appl. Polym. Sci.* 1990, **41**, 2533
15 Oleinik, E. F. *Adv. Polym. Sci.* 1986, **80**, 49
16 Kong, E. S.-W. *Adv. Polym. Sci.* 1986, **80**, 125
17 Schiering, D. W., Katon, J. E., Drzal, L. T. and Gupta, V. B. *J. Appl. Polym. Sci.* 1987, **34**, 2367
18 Gupta, V. B., Drzal, L. T., Adams, W. W. and Omlor, R. *J. Mat. Sci.* 1985, **20**, 3439
19 Gupta, V. B., Drzal, L. T., Lee, C. Y.-C. and Rich, M. J. *Polym. Eng. Sci.* 1985, **25**, 812
20 Gupta, V. B., Drzal, L. T. and Rich, M. J. *J. Appl. Polym. Sci.* 1985, **30**, 4467
21 Chang, T. D., Carr, S. H. and Brittain, J. O. *Polym. Eng. Sci.* 1982, **22**, 1213
22 Nielsen, L. E. *J. Macromol. Sci.* 1969, **C-3**, 69
23 Tager, A. 'Physical Chemistry of Polymers', Mir Publishers, Moscow, 1978, p. 170
24 Bondi, A. *J. Phys. Chem.* 1964, **68**, 441
25 Bueche, F. 'Physical Properties of Polymers', Interscience, New York, 1962, p. 103
26 Doolittle, A. K. *J. Appl. Polym. Sci.* 1951, **22**, 1471
27 Simha, R. and Boyer, R. F. *J. Chem. Phys.* 1962, **37**, 1003
28 Ferry, J. D. 'Viscoelastic Properties of Polymers', 3rd Edn, Wiley, New York, 1980, p. 201
29 Williams, M. L., Landel, R. F. and Ferry, J. D. *J. Am. Chem. Soc.* 1955, **77**, 3701
30 Simha, R. and Wilson, P. S. *Macromolecules* 1973, **6**, 908
31 Ramachandra Rao, P., Cantor, B. and Cahn, R. W. *J. Mat. Sci.* 1977, **12**, 2488
32 Meares, P. 'Polymer: Structure and Bulk Properties', Van Nostrand, London, 1965, p. 237
33 Glasstone, S., Laidler, K. I. and Eyring, H. 'Theory of Rate Processes', McGraw Hill, New York, 1941, Ch. 9
34 Hirai, N. and Eyring, H. *J. Appl. Polym. Sci.* 1958, **29**, 810
35 Perepechko, I. 'Acoustic Methods of Investigating Polymers', Mir Publishers, Moscow, 1975, p. 233
36 Kaelble, D. H., Moacanin, J. and Gupta, A. in 'Epoxy Resins: Chemistry and Technology', 2nd Edn (Ed. C. A. May), Marcel Dekker, New York, 1988, p. 603
37 Takahama, T. and Geil, P. H. *J. Polym. Sci., Polym. Phys.* 1982, **20**, 1979
38 Kumar, S. and Adams, W. W. *Polymer* 1987, **28**, 1497
39 Struik, L. C. E. 'Physical Aging in Amorphous Polymers and Other Materials', Elsevier, Amsterdam, 1978, p. 7
40 Cohen, M. H. and Turnbull, D. *J. Chem. Phys.* 1989, **31**, 1164
41 Bueche, F. *J. Chem. Phys.* 1956, **24**, 418
42 Litt, M. H. in 'Molecular Basis of Transitions and Relaxations' (Ed. D. J. Meier), Gordon and Breach, London, 1978, p. 311

43 Kanig, G. *Kolloid Z.* 1965, **203**, 161
44 Boyer, R. F. *Rubber Chem. Technol.* 1963, **36**, 1303
45 Bondi, A. 'Physical Properties of Molecular Crystals Liquids and Glasses', John Wiley, New York, 1968, p. 386
46 Kovaks, A. *J. Fortschr. Hochpoly. Forschg.* 1963, **3**, 394
47 Adamson, M. J. *J. Mat. Sci.* 1980, **15**, 1736
48 Apicella, A., Nicolais, L. and de Cataldis, C. *Adv. Polym. Sci.* 1985, **66**, 189
49 Shimazaki, A. *J. Polym. Sci., Part C*, 1968, **23**, 555
50 Storey, R. F., Dantiki, S. and Adams, J. P. in 'Cross-linked Polymers: Chemistry, Properties and Applications' (Eds R. A. Dickie, S. S. Labana and R. S. Bauer), Am. Chem. Soc., Washington DC, 1988, p. 182
51 Fisch, W., Hoffman, W. and Schmid, R. *J. Appl. Polym. Sci.* 1969, **13**, 295